

**---DRAFT---**

**SALT NIRWALS Integral Field  
Spectrograph**

**Description and Performance Predictions**

**December 2023**

**Author: Marsha Wolf (PI)**

## **1 Introduction**

Washburn Astronomical Laboratories of the University of Wisconsin-Madison Astronomy Department has developed a near infrared integral field spectrograph for the 11-meter Southern African Large Telescope (SALT), the Near InfraRed Washburn Astronomical Laboratories Spectrograph (NIRWALS). NIRWALS (originally RSS-NIR at prime focus mounted to RSS) is a standalone integral field spectrograph fed by a fiber bundle that resides inside a cold enclosure in the spectrometer room, next to the HRS enclosure (Figure 1).

This instrument is the first to extend SALT's capabilities into the near infrared, providing medium resolution spectroscopy at  $R = 2000-5000$  over the wavelength range of 800 to 1700 nm. Its integral field unit (IFU) is an elongated hexagonal bundle of 212 fibers, each of which subtends 1.3 arcsec on the sky, approximately matching the median site seeing. The IFU has on-sky

dimensions of 29 x 18 arcsec, ideally suited for resolving nearby galaxies. A separate 36-fiber bundle simultaneously samples the sky. It can be adjusted to distances ranging from 45 to 145 arcsec, but is currently telecentrically optimized for a separation distance of 97 arcsec from the object IFU. Sky fibers are interleaved with object fibers along the 8-arcmin long spectrograph slit, ultimately for optimizing sky subtraction. The spectrograph is cooled to -40 °C in an enclosure beneath the telescope, with the cryogenic dewar inside this enclosure operating at 120 K via a separate closed cycle cooler. The spectrograph uses volume phase holographic gratings with an articulated camera, similar to RSS, for setup versatility. The spectrograph has been fully tested on SALT and is now ready to begin shared risk science operation.

Instrument parameters are summarized in Table 1.



Figure 1. The NIR enclosure in the SALT Spectrometer Room (left) and the instrument inside (right). The fiber cable will enter the enclosure through the rectangular hole (currently filled with pink foam) in the upper left corner above the door. The plastic shroud around the spectrograph is to shield optical components from direct air currents from the cooling system.

Table 1. Summary of instrument parameters.

Wavelength coverage	800 – 1700 nm
Spectral resolution (R)	2000 - 5000
Peak predicted throughput	0.40
Number of fibers in IFU	212
IFU field of view on-sky	18 x 29 arcsec
Fiber size on-sky	1.33 arcsec
Number of fibers in sky bundle	36
Sky bundle field of view on-sky	4 x 29 arcsec
Adjustable sky bundle distance from IFU	45 – 145 arcsec (optimized for 97 arcsec)

# 2 Summary of Current Operational Limitations

## 2.1 Sky Subtraction

The use of simultaneously observed sky bundle fibers to subtract the sky from the object fibers is not yet implemented. Illumination variations in the SALT focal plane due to the changing pupil differentially illuminate the object and sky fiber bundles. Two efforts are actively working on this: 1) detailed modeling of the SALT focal plane via comparison to on-sky observations and 2) exploration of using the sky emission lines themselves to scale sky bundle fibers to object bundle fibers.

**Implication:** A blank sky observation should accompany every object track. This blank sky observation is scaled and used for sky subtraction in the object frame(s) by the current data reduction scripts.

## 2.2 Object and Sky Fiber Bundle Separation

Due to the current limited utility of the sky bundle for its intended purpose, we have changed the fiber bundle mounting configuration in the FIF. Previously the two bundles bisected the field center and actively tilted to the correct telecentric angles for their field distance. Now the object bundle is fixed at the center of the field and mounted normal to the focal plane. The sky bundle is mounted its FIF jaw at a fixed angle that corresponds to an optimal separation distance from the object bundle of 97 arcsec. Operation is now the same as for HRS.

**Implication:** Even though it is still possible to change the separation between object and sky bundles over the full 45 – 145 arcsec range, to optimize telecentric light coupling into the sky bundle a separation distance of 97 arcsec should be used.

## 2.3 Data Reduction Pipelines

Full data reduction pipelines are not yet implemented. UW has developed 2 data reduction scripts that are still being optimized. The first is a Python-based image processing code by Ralf Kotulla that combines multiple up-the-ramp nondestructive samples during an exposure into a flattened image with a noise extension. In the process it removes bias levels from the 32 amplifiers and does a pixel-by-pixel linearity correction. The second is an IRAF-based spectral reduction script by Matt Bershady that extracts the spectra from all fibers, performs wavelength

calibration, and does sky subtraction. The sky subtraction is still being improved. Telluric correction is not yet implemented.

Enrico Kotze at SALT has ported the IRAF spectral reduction code to a Python version.

**Implication:** Fully reduced data from a pipeline is not yet available. There are, however, early versions of data reduction scripts in Python that PIs can use to reduce their data. We encourage feedback and input to improve these scripts.

## 3 Detailed Capability Description

### 3.1 Spectral Properties

The spectrograph was designed with a suite of 4 diffraction gratings to cover the 800 – 1700 nm spectral range at all spectral resolutions. Predicted diffraction efficiency for the grating suite is shown in Figure 2 on the left. Currently, only the 950 l/mm grating is available (more gratings can be added with additional funding). Its performance is shown on the right of Figure 2. Six grating angles are required to cover the entire spectral, excluding the strong atmospheric absorption between J and H bands.

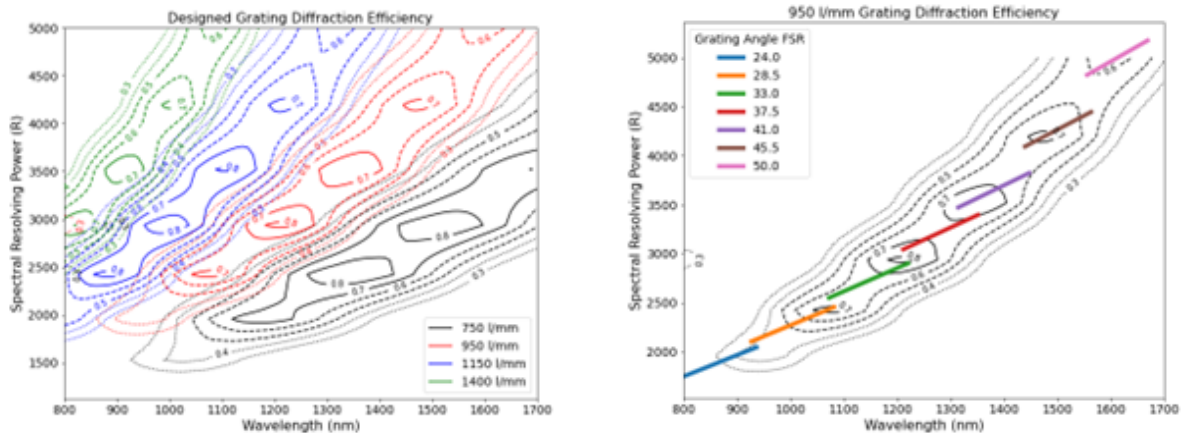


Figure 2. Predicted diffraction efficiency for the designed grating suite (left) as a function of wavelength and spectral resolution. The 950 l/mm grating performance is repeated on the right with the grating free spectral range (FSR) shown for a range of grating angles spanning the observable spectral range.

### 3.2 Instrument Throughput

The top of the atmosphere total throughput is estimated in Figure 3. This prediction includes the latest telescope throughput measured using SALTICAM on 7/4/2022 (it is down by ~10% due to a problem with the mirror coating plant). The plot is scaled to match on-sky observations with a peak of 14% at 1200 nm. The throughput falloff at both ends of the spectral range is largely dominated by the grating efficiency. This would improve with more gratings.

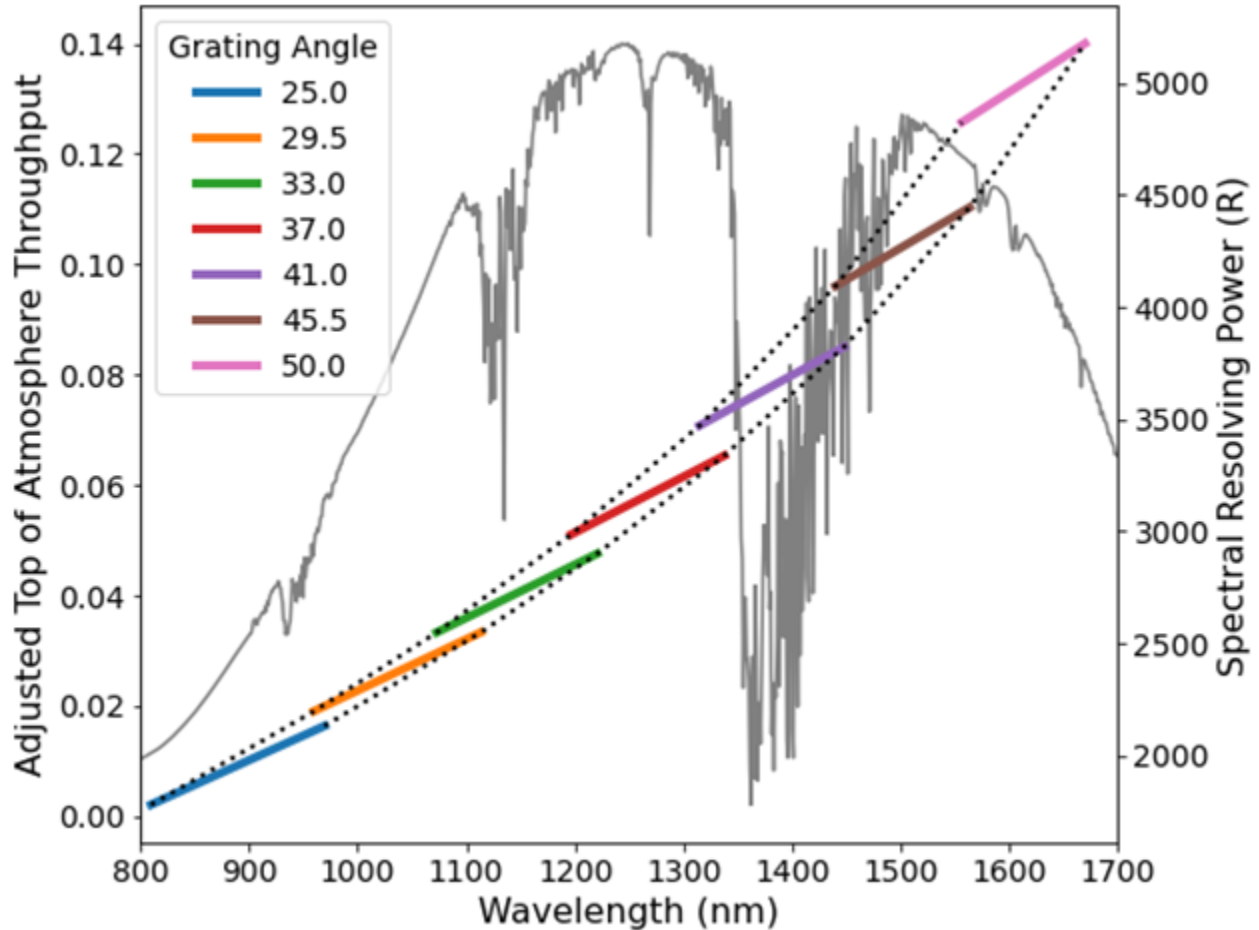


Figure 3. Top of the atmosphere throughput of the instrument and telescope (left axis). Predictions have been scaled to on-sky measurements. Grating coverage for a set of angles spanning the entire range are shown. The 41-degree angle falls within strong atmospheric absorption, so should be avoided for typical setups. Excluding that region, the entire range can be covered with 6 instrument configurations. Spectral resolution as a function of wavelength (and grating angle) is shown on the right axis.

### 3.3 Predicted Performance

The night sky spectrum in the near infrared is filled with bright OH emission lines. A spectrum from Mauna Kea is shown in Figure 4. These emission lines add significant noise, limiting achievable S/N at their spectral locations. Estimated mean S/N per spectral resolution element

for an extended source filling the fiber is given in Figure 5 as a function of object magnitude for an 1800 sec exposure, and Figure 6 gives limiting magnitudes between the sky lines for mean S/N~5 in 1800 sec. Figure 7 shows the predicted S/N spectra for each grating setting for a 21<sup>st</sup> magnitude object.

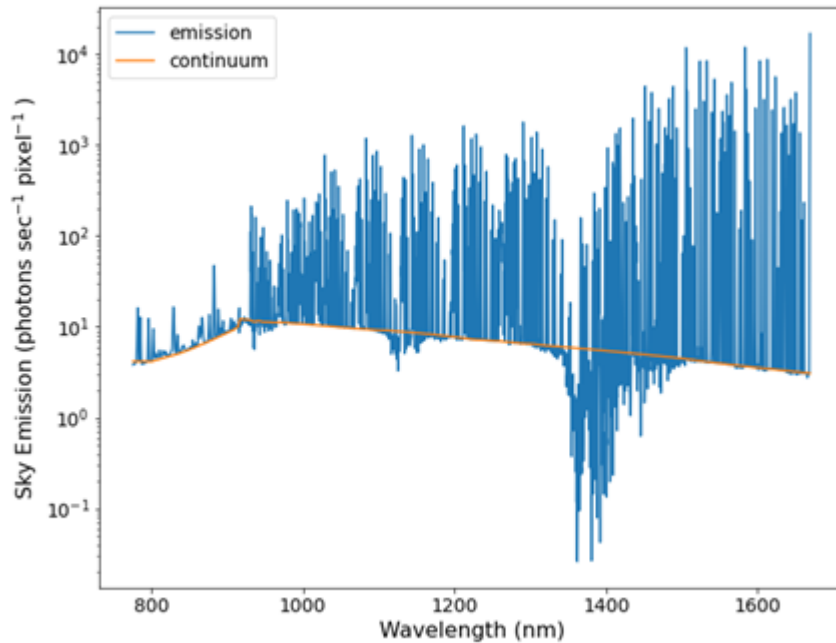


Figure 4. Sky emission spectrum from Maunaea Kea. It has been smoothed to the NIR instrumental spectral resolution.

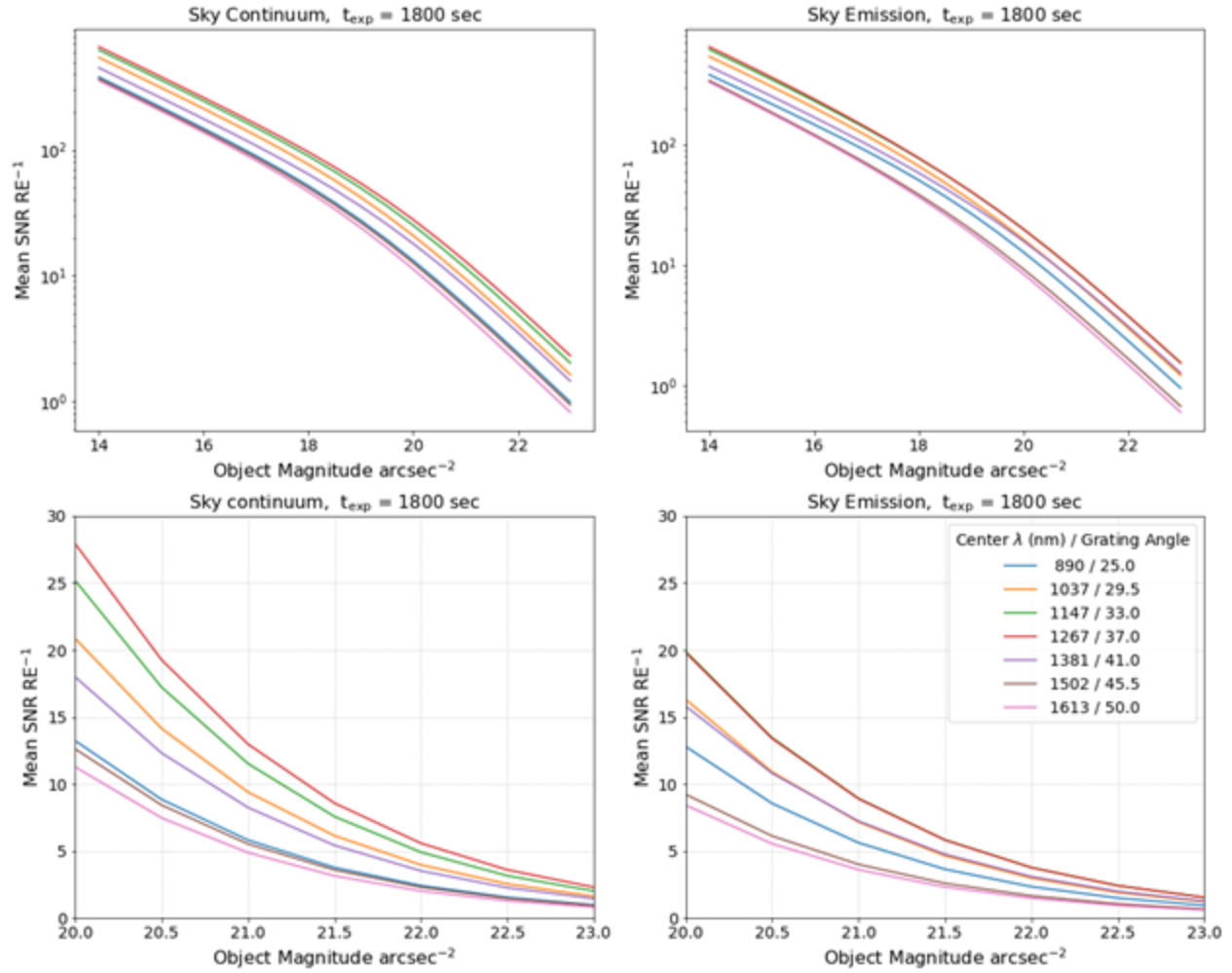


Figure 5. Estimated mean S/N per resolution element for an extended source filling the fiber, as a function of object magnitude, for an 1800 sec exposure. Plots on the left are for the sky continuum regions free of bright sky emission lines. Plots on the right are mean values over the entire grating FSR, including sky emission line regions. These plots use on-sky-measured system throughput.

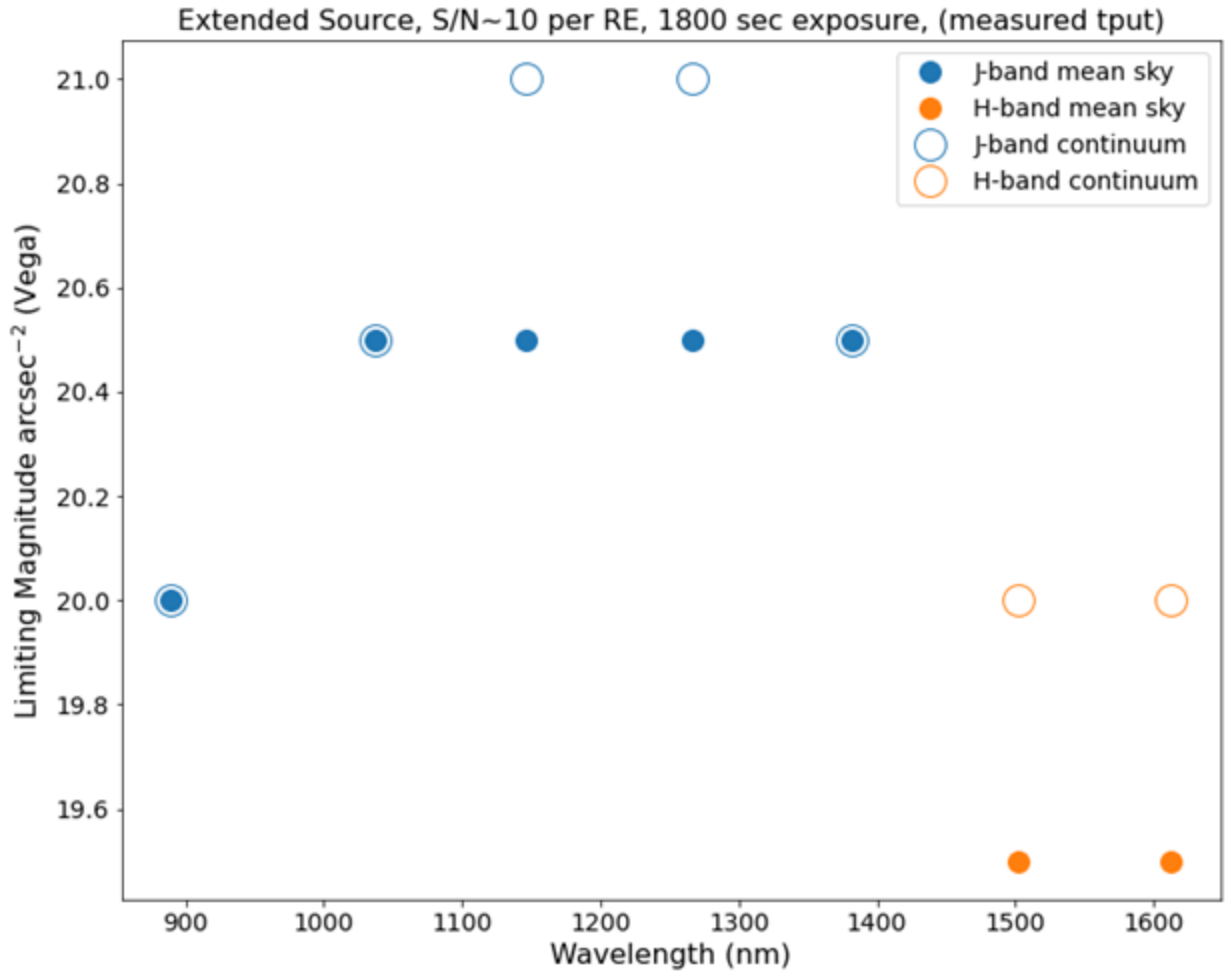


Figure 6. Estimated limiting magnitudes for mean S/N ~ 10 in an 1800 sec exposure.



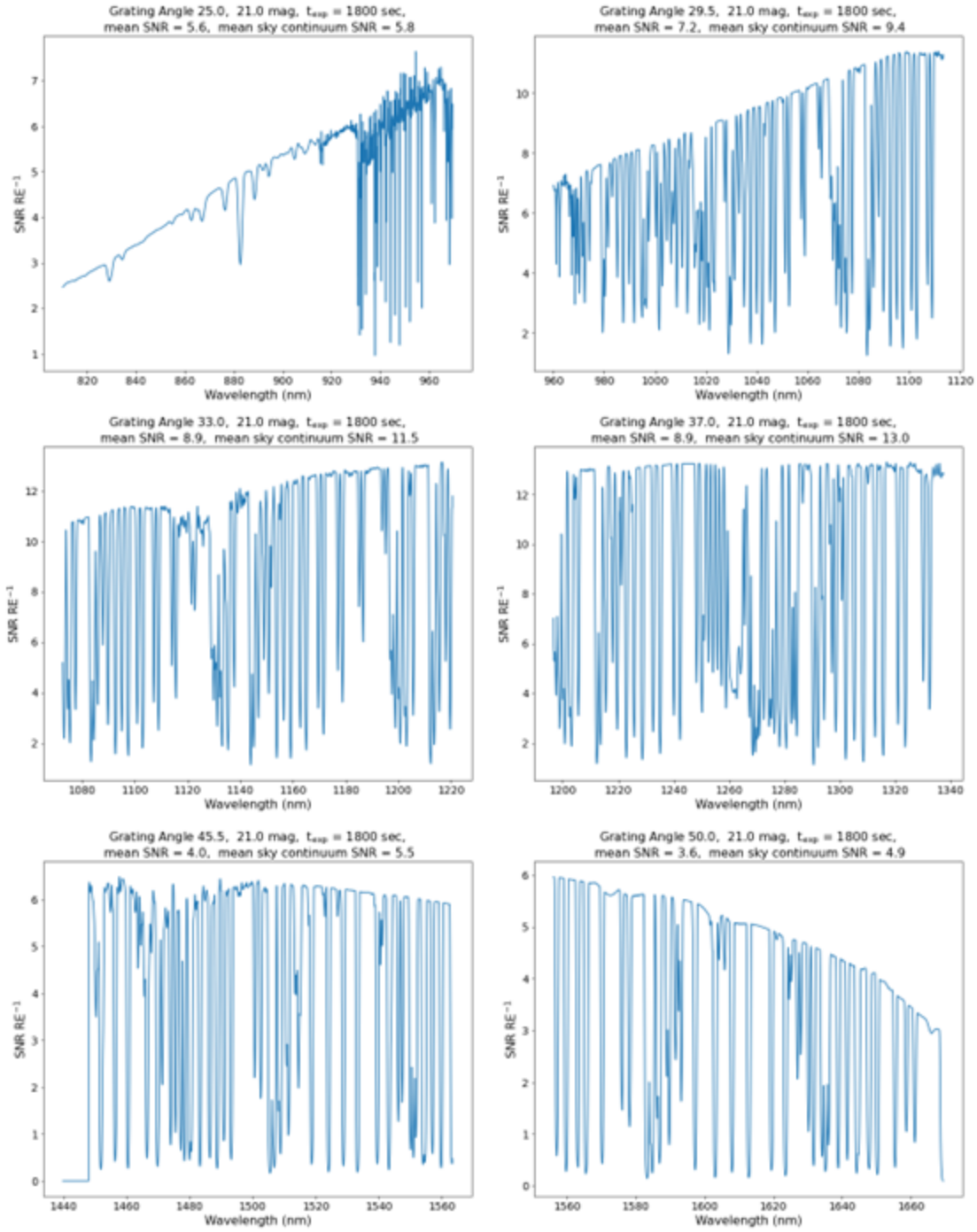


Figure 7. Estimated S/N per resolution element in each of the 6 grating settings (grating angle is listed in the title of each panel) for a 21<sup>st</sup> magnitude extended object. The panel titles give the mean S/N for both the full spectral range and for just the emission line-free continuum regions.

## 4 Integral Field Unit

The integral field unit contains 212 object fibers. Its extent on the sky is 29 x 18 arcsec. A separate sky bundle contains 36 fibers (2 of 38 fibers were broken during construction), with an extent on-sky of 4 x 29 arcsec. The layouts are shown on the left of Figure 8. These fiber ferrules are mounted in the SALT fiber instrument feed (FIF), which also holds fibers that feed the HRS (Figure 8, right). The object IFU is mounted in the top jaw and the sky bundle in the bottom jaw. The distance between the two is adjusted by moving the jaws apart. This separation distance range is 45 to 145 arcsec, but telecentric light coupling into the sky bundle fibers is optimized at a separation of 97 arcsec.

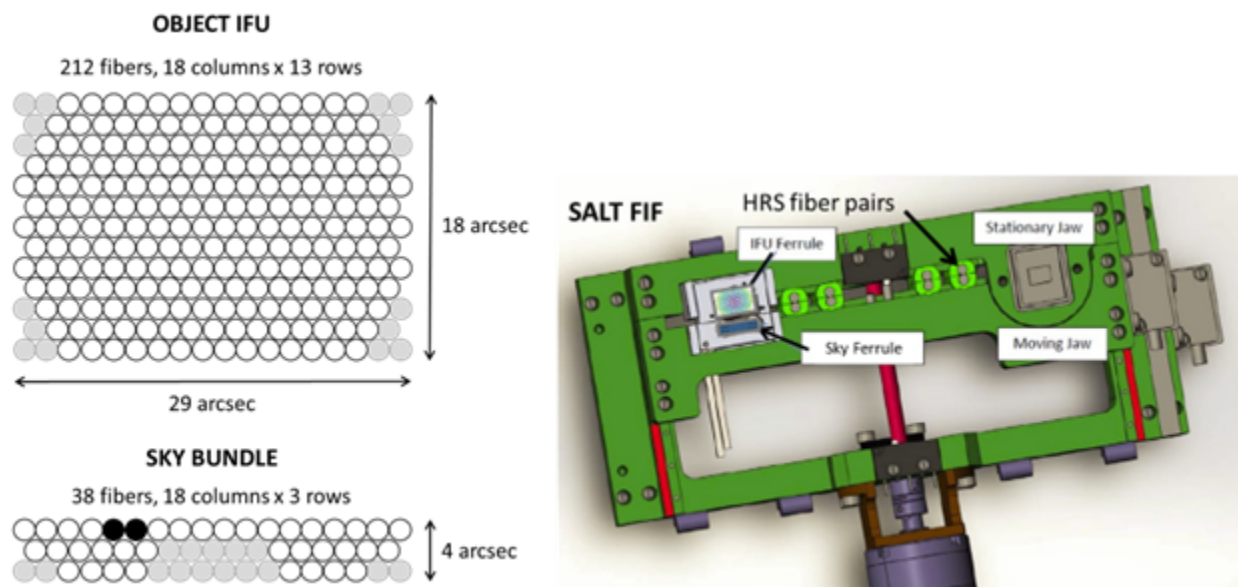


Figure 8. Layout of the object IFU and the sky bundle (left). Gray fibers are unused and black fibers are broken. Mounting of the ferrules in the SALT fiber instrument feed (right). The FIF jaws separate, providing an adjustable distance between the sky bundle and the object IFU.

The FIF is now used in the same mode as for HRS, placing the object bundle at the center of the SALT optical field the sky bundle is separated from that by a specified distance. Both bundles are mounted at fixed angles: 0 degrees for the object bundle at field center and an angle corresponding to a field distance of 97 arcsec for the sky bundle. The telecentric angle on SALT changes by 78 arcsec angle per arcsec of field distance. Because the IFU has a fixed size the fibers at the edges will have some telecentric angle offset relative to the center. This is shown in Figure 9. The arrangement of the sky bundle was designed to reproduce this distribution of telecentric angle errors. Object and sky fibers with similar telecentric errors are placed together along the slit.

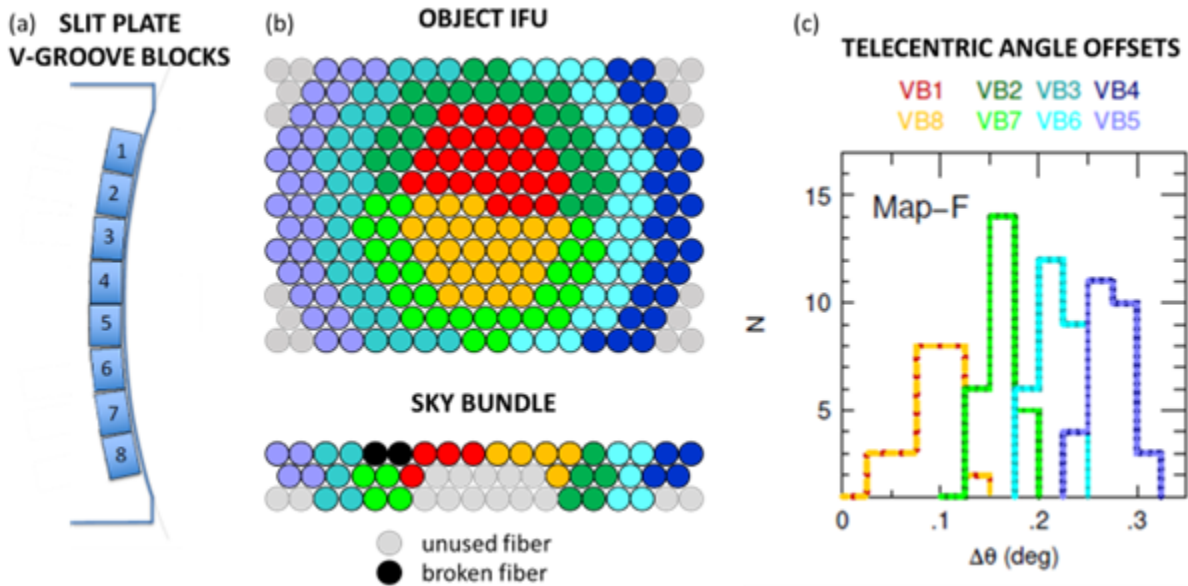


Figure 9. Fiber telecentricity considerations. (a) Fibers are arranged into a spectrograph entrance slit consisting of 8 V-groove blocks that range from 30 to 32 total fibers each (including 4-5 sky fibers). (b) Arrangement of object IFU and sky bundle fibers into slit blocks. The colors denote different V-groove blocks (VBx). (c) Telecentric angle offsets for fibers in the object IFU that map to labeled VB's in the slit. The sky bundle arrangement was designed to sample this distribution of offsets. Sky fibers and object fibers with similar telecentric angle errors are placed together along the slit.

## 5 Detector System

The NIR detector is a Hawaii-2RG, 2048 x 2048 array with 18-micron pixels. Two modes are planned for faint and bright objects. Currently, only the faint mode is optimized and available. Relevant parameters measured in the laboratory for each mode are given in Table 2. Sampling modes for NIR detectors include correlated double sampling (CDS), Fowler sampling, and up-the-group-ramp (URG). Multiple sampling modes are explained in Figure 10. In Fowler sampling mode, reads at the beginning are averaged, reads at the end are averaged, and the two averages are subtracted. In URG mode, a slope is fit to the group reads up-the-ramp to reduce noise in the individual reads.

NIRWALS operation is currently limited to the URG sampling mode. All exposures are automatically nondestructively sampled at the frame rate (0.72775 sec). This is necessary for proper pixel linearity and dark current calibration due to detector degradation.

About 11% of the pixels in the detector have degraded operability and show up as "hot" pixels. This is due to a design flaw in Teledyne detectors of that era, which allowed indium from the

bump bonds to interdiffuse with the gold in the contact structure and migrate into the HgCdTe pixel material. The result is much higher dark current in the affected pixels, which appears to be time dependent and nonlinear. Work is ongoing to determine how many of these pixels are usable for science and the appropriate pixel masks will be made.

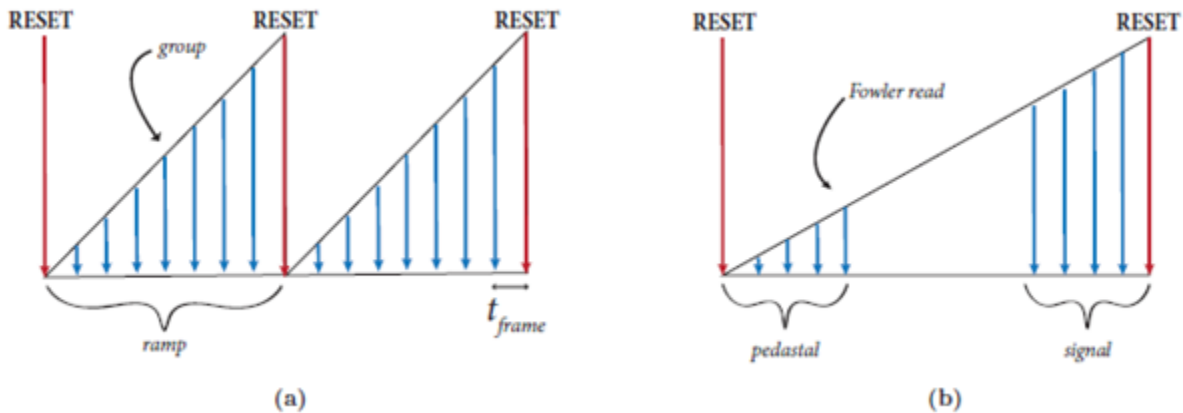


Figure 10. Detector sampling modes: up-the-ramp group sampling (left) and Fowler sampling (right). The vertical dimension represents accumulated signal in a pixel, and the horizontal dimension represents time, increasing to the right. Downward arrows represent times that the detector array is nondestructive read in groups up the ramp or in Fowler sampling at the beginning and end of a ramp.

Table 2. Detector parameters measured during laboratory optimization.

Readout channels	32	
Pixel sampling speed	200 kHz	
Frame readout time	0.72275 sec	
<b>Measured</b>	<b>faint mode: 18 dB preamp gain</b>	<b>bright mode: 9 dB preamp gain</b>
Conversion gain	2.04 e-/DN	5.49 e-/DN
CDS read noise (all pixels)	24.6 +/- 6.2 e-	40.1 +/- 9.3 e-
Full well depth	83,500 e-	158,770 e-
Amplifier crosstalk	~7 E-04	
<b>Estimated</b>		
Read noise Fowler-64(4)	7.6 e- (19.8 e-)	11.7 e- (30.3 e-)
Read noise URG-100(15)	13.8 e- (22.7 e-)	20.6 e- (33.7 e-)

NOTE: Fowler-64 has 64 reads at the beginning and end, URG-100 has 100 reads up the ramp during an exposure.

## 6 Observing Modes

Envisioned observing modes include two main scenarios.

### 6.1 FIF Offsets

These offsets are used when small dithers ( $\leq 3$  fiber diameters) are required to improve background subtraction in point source observations (Figure 11) and for “filling in the gaps between fibers” for mapping observations. They will also be used to map small extended targets (smaller than the IFU FOV). These will involve movement of the FIF stage. The movements will have a very high positional accuracy:  $\leq 0.1$  arcsec, the lowest overheads of the offset modes, but they will be limited to small offsets ( $< 5$  arcsec) to avoid non-telecentricity effects.

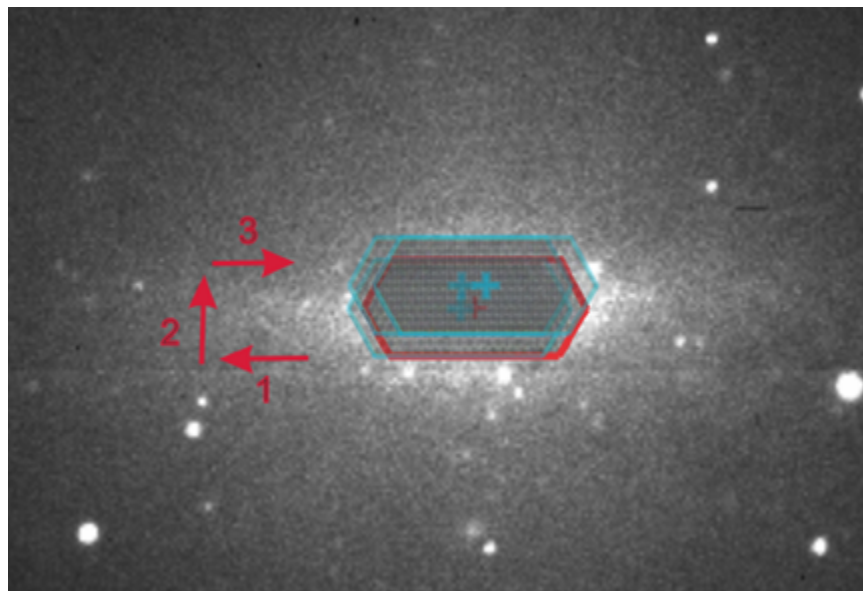


Figure 11. Illustration of NIR IFU science bundle positions and offsets for a small extended source that requires small dithers to better sample the field. The NIR IFU science bundle FOV (in the science and sky/offset positions) and central position overlays are shown in red, the offset directions are shown in cyan with an extended source in the background.

### 6.2 Tracker Offsets

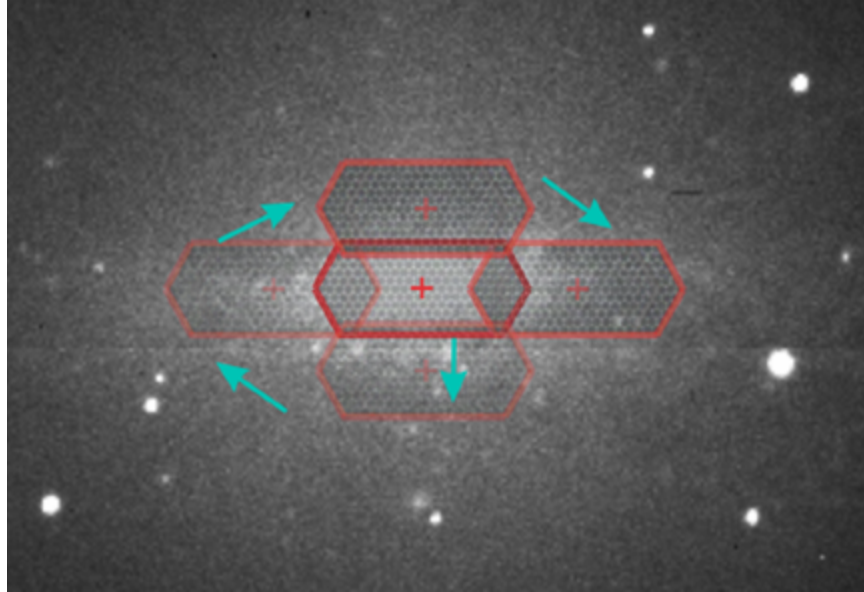


Figure 12. Illustration of NIR IFU science bundle positions and offsets for a large extended source that requires large dithers. The NIR IFU science bundle FOV (in the science and sky/offset positions) and central position overlays are shown in red, the offset directions are shown in cyan with an extended source in the background.

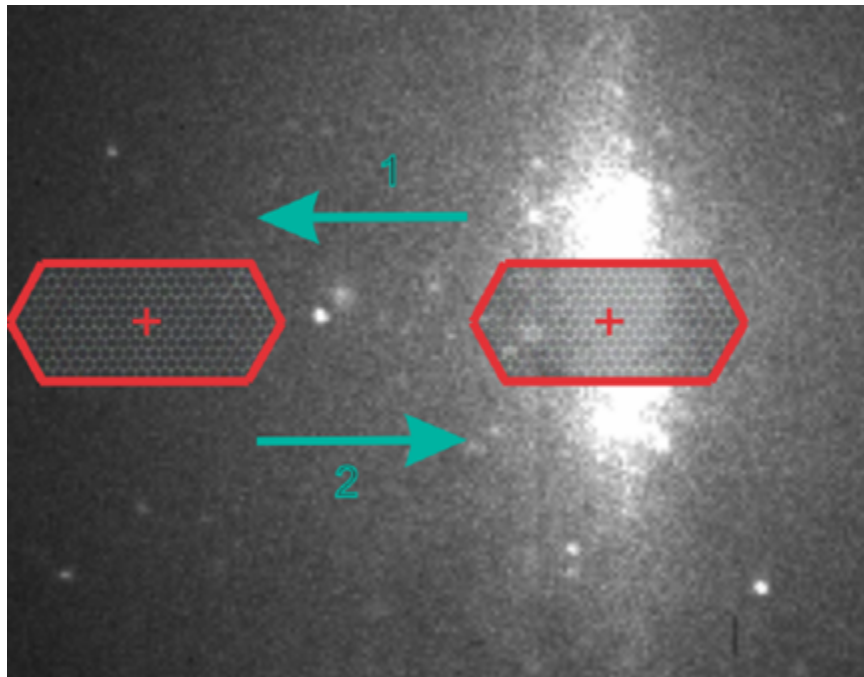


Figure 13. Illustration of NIR IFU science bundle positions and offsets for an extended source that requires large dithers. The NIR IFU science bundle FOV (in the science and sky/offset positions) and central position overlays are shown in red, the offset directions are shown in cyan with an extended source in the background.



### 6.2.1 Guided

These consist of tracker movements with guidance maintained after the offset is made. The moves will have positional accuracy of  $\leq 0.2$  arcsec (dependent on the seeing) and limited to offsets of up to  $\sim 90$  arcsec. The overheads will include the time required for the tracker movement and time waiting for the guidance to settle after the tracker movement. This will be the workhorse offset mode and will be utilized for blind acquisition offsets, for dithers to improve sky subtraction and for mosaicing large objects.

## 7 Calibration

SALT has a separate calibration bay for NIR. It contains a QTH flat field lamp and 3 penray arc lamps: Argon, Neon, and Krypton. The lamps all mount into an integrating sphere, allowing any of them to be selected individually or simultaneously. A set of neutral density filters are also available for tuning calibration exposure times. A new near infrared liquid light guide transports the lamp light to the existing calibration system Fresnel lenses that are designed to reproduce the SALT vignetting pattern. The Fresnel lens material is acrylic, in which throughput significantly drops beyond a wavelength of 1600 nm. SALT is planning a Phase II calibration system upgrade that will address this issue while also improving throughput in the blue for other instruments (potentially with an all reflective optical relay system).

Even so, sufficient QTH flat field light reaches NIRWALS to trace spectra through the reddest configuration with the 950 l/mm grating at 50-degrees, as shown in Figure 14.

The stability of wavelength solutions on arc lamp spectra collected at different times with different instrument configurations was analyzed by Moses Mogotsi using Enrico Kotze's pipeline wavelength calibration. The wavelength zeropoint RMS is in the range of 0.5-1 pixel, which is a velocity error of 15-30 km/s in the blue ( $g=25$ ) setup and half that in the  $g=37$  setup. Results from Mogotsi's report are shown in Figure 15.

**Implication:** Measured repeatability is sufficient for some science, meaning that calibrations would not need to be taken with the observation. The option to take charged calibrations with the science observation (as is done on RSS) can be selected in the PIPT if higher wavelength precision is required.

**Darks** should be taken the same night as observations.

It is recommended to observe a **telluric standard star** following each science target track. It should be as close as possible to the same part of the sky as the science target.

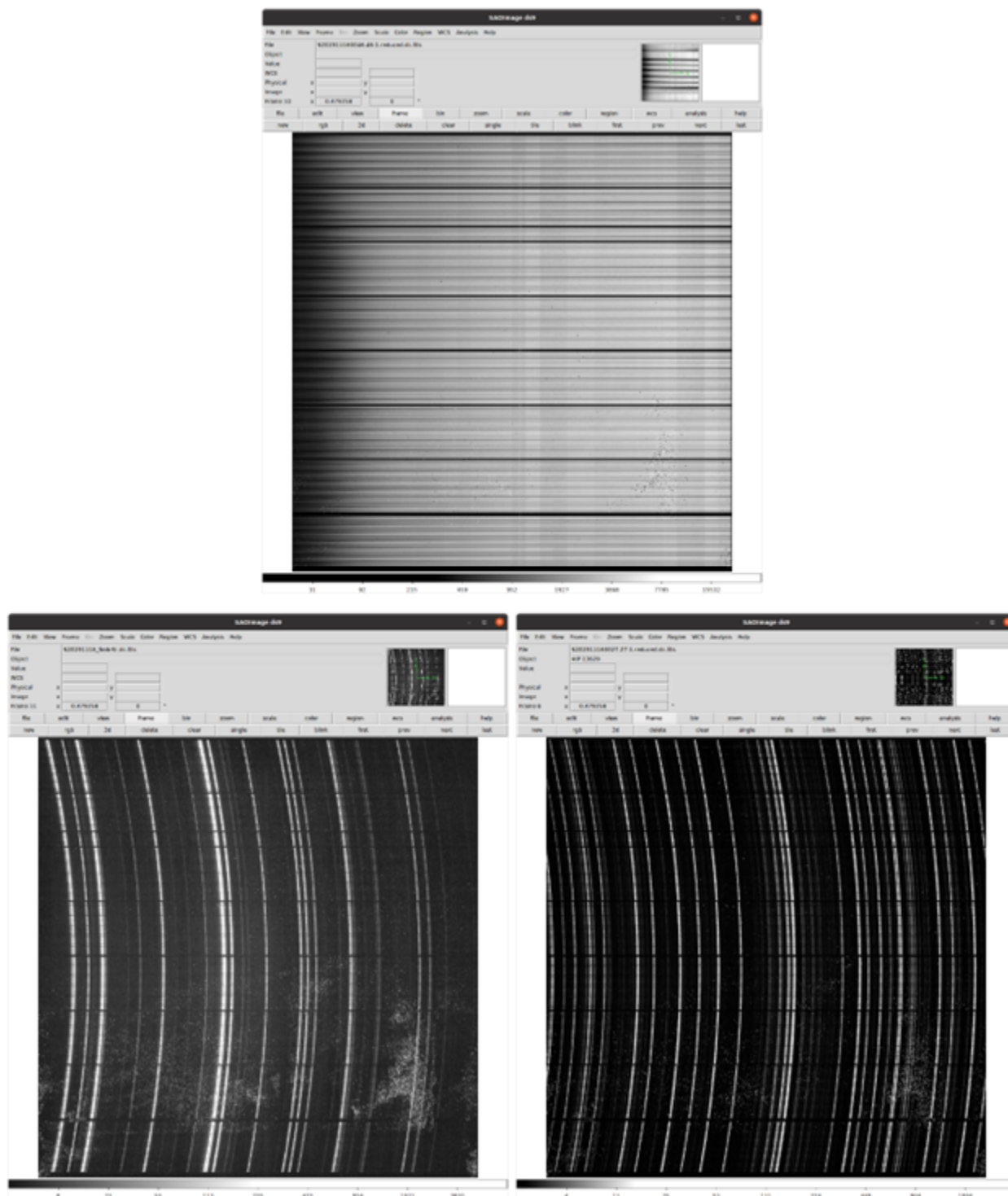


Figure 14. Calibration frames in the reddest NIRWALS configuration with the grating at 50-degrees. Redder wavelengths are on the left edge of the images. The images are the QTH lamp (top), combined Ne, Ar, Kr arc lamp images (bottom left), and a blank sky image (bottom right).



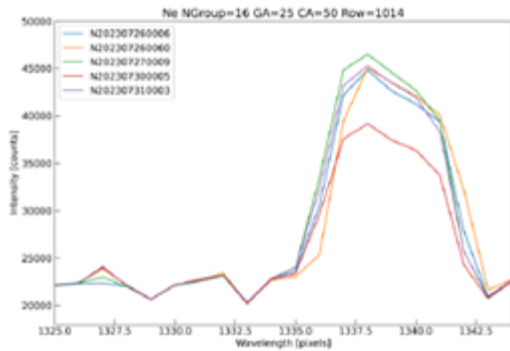


Figure 1a: Ne arc line data from row=104 of raw Ne GA=25, CA=50 arc images taken between 26-31 July

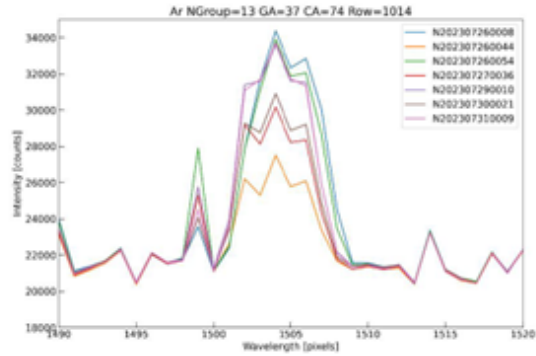


Figure 3c: Ar arc line data from row=1014 of raw Ar GA=37, CA=74 arc images taken between 26-31 July

Figure 15. Stability of the same arc lines observed with spectrograph reconfiguration on different days.

## 8 Observations

### 8.1 Acquisition

Target acquisition is performed using SALTICAM and the FIF acquisition camera. It is done in the optical, therefore optical finder charts of targets or reference objects should be provided for the acquisition process. Acquisition is similar to the process followed for the HRS instrument and the same guidance system is used, therefore the acquisition overheads are expected to be similar (600s). As mentioned in Section 2.1 and 2.2, the default science and sky fibre bundle separation has been optimized for 97 arcsec, and that is the default separation distance.

The FIF Acquisition camera is an optical camera and it is not ideal for the acquisition of faint targets. PIs that would like precise acquisition of diffuse or faint ( $V > 16$ mag) are advised to use reference stars that will be used for acquisition.

### 8.2 Dither Offset/Setup

The Dithers and Offsets (e.g., for sky offset) can be specified in the PIPT, in the format below:

Bundle Separation  arcsec

Dither pattern

#	Offset Type	X Offset	Y Offset	Exposure Ti...	Gain	Sampling	Reads	Ramps	Groups
1	FIF Offset	0.0	0.0	600.0	Faint	Up-the-Ram...	1	1	824
2	Tracker Gui...	60.0	0.0	600.0	Faint	Up-the-Ram...	1	1	824

Each dither step consists of an offset (either FIF or Tracker Guided) and an exposure setting. During observations these offsets and exposures are performed automatically, with the offset in each dither step performed before the exposure. The overheads for each offset type are still

being determined, however PIs are advised to use conservative overhead calculations similar to the RSS offsets overheads.

### **8.3 Exposure Setups**

The shortest exposure time will be for an image taken with two reads: ~1.5 sec. The maximum sampling rate (0.728s) will be used for all data. And PIs should be aware that individual exposures longer than 10min are not advisable due to the variability of the near-infrared sky. Instead, long exposures should be broken up into shorter ones.

Extensive testing data has only been taken for the following configurations:

Grating Angle (GA)=25 deg, Camera Angle(CA)=50 deg;

Grating Angle=29.5 deg, Camera Angle=59 deg;

Grating Angle=37 deg, Camera Angle=74 deg

Grating Angle=50 deg, Camera Angle=100 deg

These cover most of the wavelength range of the instrument, and calibrations have only been tested for these setups.

### **8.4 Calibrations**

PIs need to determine whether their science will require charged or uncharged arcs (see Section 7). Only 4 setups were tested, and for two of these setups, and of these GA=29.5 and GA=50 required either separate exposures of all four arc lamps. In the latter case sky lines seem the most reliable manner to calibrate the data. These require up to an additional 120s for the calibrations. We advise PIs to add an additional 120s overhead for GA settings in between the tested ones.

If PIs require telluric standards to be taken before or after their science observations, they need to select the specific star they would like to observe and they need to create a separate observing block for the Telluric standard. The total time for these telluric star observations standards will be charged.

Darks will be taken on the same night as the data and will be uncharged.

Spectrophotometric standards will be taken on a regular basis for the particular setups that are observed.

## **8.5 Data Reduction**

As mentioned in Section 2.3, a python-based data reduction pipeline is being developed (that follows the same procedures as the IRAF-based procedures developed by UW), and it will run after the pre-processing of the data into a 2-D fits file. Various aspects of the data processing and data reduction pipeline will continue to be developed and refined. We expect that an early version of the pipeline will be running when the data for this call is taken.